



## Microwave Synthesis and Characterization of Multiwalled Carbon Nanotubes (MWCNT) and Metal Oxide Doped MWCNT

A. Lakshmi<sup>1,2,\*</sup>, D. Lydia Gracelin<sup>2</sup>, M. Vigneshwari<sup>2</sup>, P. Karpagavinayagam<sup>2</sup>, V. Veeraputhiran<sup>2</sup>, C. Vedhi<sup>2</sup>

<sup>1</sup>Department of Chemistry, St. Mary's College, Tuticorin – 628 001, TN, India.

<sup>2</sup>Department of Chemistry, V.O Chidambaram College, Tuticorin – 628 008, TN, India.

### ARTICLE DETAILS

#### Article history:

Received 12 July 2015

Accepted 27 August 2015

Available online 12 September 2015

#### Keywords:

Multiwalled carbon nanotubes (MWCNT)

Metal Oxide

Microwave

Sonication

Impedance

### ABSTRACT

Multiwalled carbon nanotubes (MWCNT) and metal oxide doped (MWCNT/MO) was synthesized using domestic microwave oven and characterized by UV-Visible, XRD impedance, polarization and AFM studies. In UV-Visible spectrum of MWCNT there are two peaks in the region 733 nm, and 340 nm attributed to  $S_{22}$  transition taking place in carbon nanotubes and  $\pi \rightarrow \pi^*$ . Metal oxide doped MWCNT exhibits their respective M-L transition bands. The band gap energy was calculated using Tauc's plot and it was found to be best for MWCNT-CuO nanocomposite. XRD studies revealed the formation of MWCNT/MO nanocomposite. The XRD pattern obtained for MWCNT/MO nanocomposite was in good agree with JCPDS file. From the impedance studies it was clear that charge transfer resistance ( $R_{ct}$ ) value increased when a metal oxide was doped into MWCNT. It was also confirmed in Tafel studies that polarization resistance was increased for MWCNT/MO nanocomposite. The surface morphological behaviour was studied by AFM technique. It showed the formation spherical shaped nanocomposites.

### 1. Introduction

The field of nanotechnology has experienced a constantly increasing interest over the past decades both from industry and science. Since the accidental discovery of carbon nanotubes (CNTs) during the synthesis of fullerene by Iijima [1], tremendous research has been done on CNTs. CNTs are under intense investigation owing to their spectacular mechanical and electrical properties [2]. Many ways are currently available for the production of CNTs, which are arc-discharge [3], pulsed laser vaporization [4], chemical vapor deposition [5]. However, commercial applications of CNTs have been inhibited by the lack of large-scale production of purified CNTs. Moreover, the intrinsic Vander Waals attraction of CNT's towards each other leads easily to entangle agglomerates, which results in their insolubility in most of organic and aqueous solvents. Recently, a microwave-assisted synthesis is enabling technology that has been extensively used in organic synthesis [6-8]. Microwave-assisted modification of CNTs is non-invasive, simple, fast, environmentally friendly, and clean method as compared to traditional methods. Usually, the use of the microwave facilitates and accelerates reactions, often improving relative yields. In case of microwave-assisted functionalization of CNTs, microwave irradiation of CNT reduces the reaction time and gives rise to products with higher degrees of functionalization than those obtained by the conventional thermal methods [9]. A wide range of metals, such as are gold [10], platinum, ruthenium [11], rhodium [12] and copper [13] have been incorporated. It is of current general interest the development of new techniques for the efficient and selective synthesis of CNT's and other carbon nanostructures at the cheapest possible cost. One such possibility is the use of microwave radiation, which over the past few years has played an important role as a thermal tool in organic synthesis due to considerable advantages over conventional methods. Kharissova has reported the synthesis of vertically aligned carbon nanotubes using a domestic microwave oven [14]. The use of microwave radiation in the synthesis and functionalization of carbon nanotubes or other nanostructures is advantageous because it provides a fast and uniform heating rate that can be selectively directed towards a targeted area. In the present study we have doped some metal oxides in to MWCNT using surfactant by sonication method.

### 2. Experimental Methods

#### 2.1 Materials

All reagents were of analytical grade and used as received without further purification. Ultra-pure deionized water was used throughout the experiments. Graphite (Micro Fine Chemicals), Cetyl trimethyl ammonium bromide (CTAB), cobalt chloride (Merck), copper sulfate (Merck), nickel sulfate (Merck), ethanol, iron (II) acetate (Merck) were purchased and used in the synthesis.

#### 2.2 Synthesis of MWCNT

Starting material was prepared by mixing 3 g of iron (II) acetate with 7 g graphite powders. The powders were then mixed and placed inside domestic microwave oven and irradiated inside at 700 W until microwave oven reaches about 1000 °C for 12 seconds.

#### 2.3 Functionalization of MWCNT

The MWCNTs are dispersed in 10 mL ethanol then 30 mL of 0.1 M CTAB was added for dispersing the MWCNT. The dispersion was achieved by sonicating the mixture for 30 minutes.

#### 2.4 Synthesis of MWCNT/Metal Oxide Nano Composite

The precursor of the metal oxide is separately dissolved in deionized water. Then, metal oxide solution drop-wise added into the dispersed MWCNT's and the mixture is sonicated and magnetically stirred for 1 h. After that, the suspensions mixture is transferred into round-bottomed flask and refluxed at high temperature 120 °C. After that, the system is allowed to cool at room temperature. Then, the mixture is filtered and washed with suitable solvent like distilled water and ethanol several times. The resulted composite is dried at 100 °C. The end product embedded with nano-sized metal oxide was collected and characterized.

### 3. Results and Discussion

#### 3.1 UV- Visible Spectral Studies

The UV-Visible spectrum of carbon MWCNT and MWCNT/MO nanocomposites (figures not given) shows two peaks for MWCNT in the region 733 nm, and 340 nm. It is due to  $S_{22}$  transition taking place in carbon nanotubes and  $\pi \rightarrow \pi^*$  transition of  $\pi$  electrons present in MWCNT. In the

\*Corresponding Author

Email Address: [magathalenalakshmi@yahoo.co.in](mailto:magathalenalakshmi@yahoo.co.in) (A. Lakshmi)

spectrum of MWCNT/Co<sub>3</sub>O<sub>4</sub>, the spectrum has three distinct peaks at 730 nm, 400 nm and 290 nm. The peak at 730 nm is due S<sub>22</sub> transition taking place in CNT. The peak at 290 nm is assigned to the O<sup>2-</sup> → Co<sup>3+</sup> charge transfer [15]. The peak at 730 nm in the UV spectrum of MWCNT/ NiO is assigned to the S<sub>22</sub> transition of CNT. The peak at 290 nm is due to π → π\* and 300 nm is due to the NiO transition. In the spectrum of MWCNT- CuO, the peak at 730 nm similar to other peaks due to S<sub>22</sub> transition of CNT. The peak at 310 nm is due to π → π\* transition. The peak at 400 nm is due CuO.

### 3.2 Band Gap Energy

The measurement of the band gap of materials is important in the semiconductor, nanomaterial and solar industries. The term “band gap” refers to the energy difference between the top of the valence band to the bottom of the conduction band electrons are able to jump from one band to another. In order for an electron to jump from a valence band to a conduction band, it requires a specific minimum amount of energy for the transition, the band gap energy. The band gap energy of insulators is large (>4 eV), but lower for semiconductors (<3 eV). Diffuse Reflectance UV-Vis spectroscopy involves numerous light-sample interactions, spectra may exhibit features associated with the transmission and/or reflection (external and/or internal) of UV-Vis radiation. From the reflectance spectrum band gap energy was calculated using Tauc plot and given in Table 1.

**Table 1** Band gap energies of MWCNT and its metal oxide composites

Sample	Band gap energy (eV)
MWCNT	1.82
MWCNT-Co <sub>3</sub> O <sub>4</sub>	1.71
MWCNT-NiO	1.70
MWCNT-CuO	1.693

### 3.3 X-Ray Diffraction Studies

XRD is used to ascertain the quality and crystalline nature of nanotubes. Fig. 1 shows the X-rays diffraction pattern of MWCNT-Co<sub>3</sub>O<sub>4</sub>. The pattern shows the intense peak at 2θ=25.9° is due to (002) reflection. The other peaks at the angles 2θ of 44.6°, 49.4°, 54.5° and 62.4° are due to the (100), (101), (004) and (110) reflection. The peaks at 23.8°, 33.12°, 35.6°, 40.83°, 44.52°, 59.84°, 63.9° obtained for Co<sub>3</sub>O<sub>4</sub> is similar to cubic structure of Co<sub>3</sub>O<sub>4</sub> [16] with lattice constant a=3.52 Å. The average grain size of MWCNT - Co<sub>3</sub>O<sub>4</sub> is 57.7 nm. Fig. 2 shows the XRD pattern of MWCNT-NiO. In this in addition to diffraction pattern of MWCNT the additional peak at 33.11°, 35.58°, 54.6°, 87.01°, 87.27° corresponds to (111), (200), (220), (311) and (222) planer of face-centered cubic [FCC] crystallite phase of NiO [17]. (JCPDS file No. 04-0835) with lattice constant a=3.648 Å. The average grain size of MWCNT-NiO is 86.88 nm. XRD pattern of MWCNT-CuO nano composite is shown in Fig. 3. It gives a single phase with monoclinic structure. The peak at 33.2°, 49.4°, 54.5°, 62.4° which corresponds the (002), (202), (020) and (113) planes. This is in good agreement with reported refracted values of CuO [18]. (JCPDS No.05-661) with lattice constant a=3.582 Å. The average grain size of MWCNT-CuO is 82.03 nm.

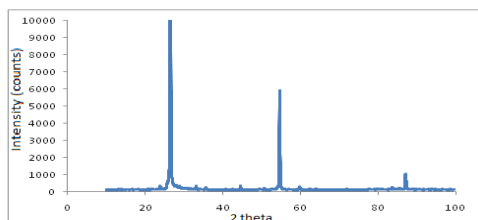


**Fig. 1** XRD behavior of MWCNT-Co<sub>3</sub>O<sub>4</sub>

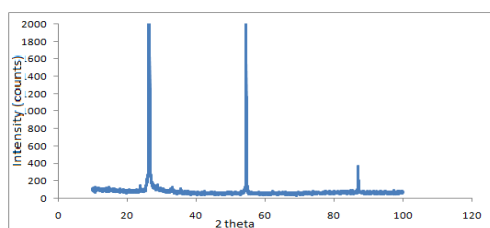


**Fig. 2** XRD behavior of MWCNT-NiO

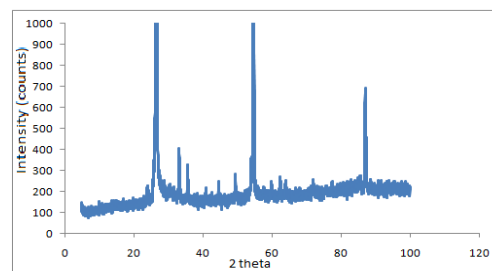


**Fig. 3** XRD behavior of MWCNT-CuO

### 3.4 Cyclic Voltammetric Studies

The LUMO of MWCNT can accept six electrons to form hexaanion. But here we were reporting three electron oxidation-reduction mechanism. The reason for that is functionalization reduces the redox behavior of MWCNT (Fig. 4). The cyclic voltammetric behavior of MWCNT-Co<sub>3</sub>O<sub>4</sub> was given in Fig. 5 The cathodic peak at -0.28 was due to the reduction of Co<sup>2+</sup>. This was the standard reduction potential of Co<sup>2+</sup>. Fig. 6 shows the redox behavior of MWCNT-NiO. Here Ni<sup>2+</sup> under goes oxidation around 0.25 V and this anodic peak merges with redox peak of MWCNT and forms a broad peak. In the case of CuO nanocomposite (Fig. 7) additional to the redox nature of MWCNT, the anodic peak at 0.4 V was due to the oxidation of Cu<sup>2+</sup>.

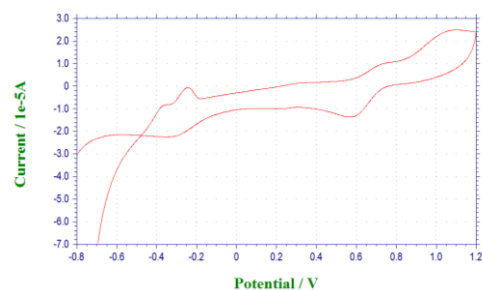


**Fig. 4** Cyclic voltammetric behavior of MWCNT in pH 1.0 at a scan rate of 50 mV/s

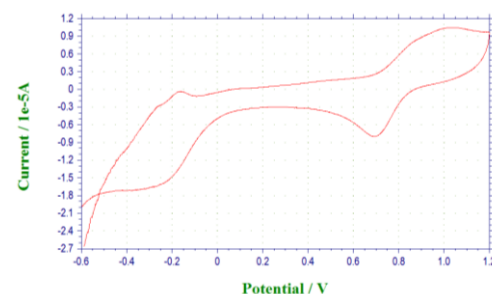


**Fig. 5** Cyclic voltammetric behavior of MWCNT-Co<sub>3</sub>O<sub>4</sub> in pH 1.0 at a scan rate of 50 mV/s

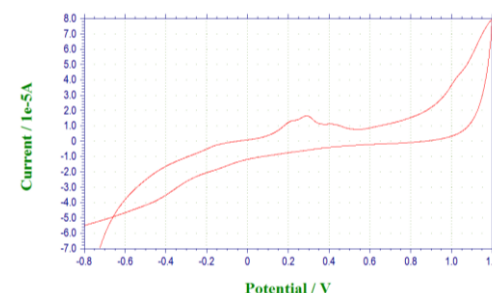


**Fig. 6** Cyclic voltammetric behavior of MWCNT-NiO in pH 1.0 at a scan rate of 50 mV/s

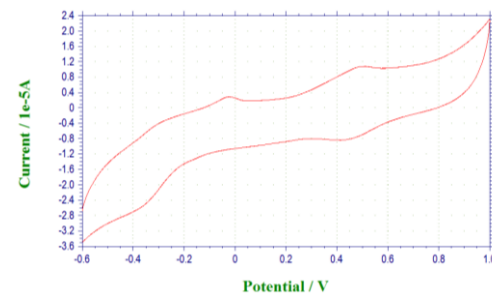


**Fig. 7** Cyclic voltammetric behavior of MWCNT-CuO in pH 1.0 at a scan rate of 50 mV/s

### 3.5 EIS and Polarization Studies

Electrochemical impedance spectrum (Fig. 8) was studied using GCE modified with MWCNT, MWCNT-Co<sub>3</sub>O<sub>4</sub>, MWCNT-NiO, MWCNT-CuO (0.0314 cm<sup>2</sup>) as working electrode. The cell contains a 1 cm<sup>2</sup> Pt counter electrode, Ag/AgCl reference electrode. The measurements were carried out in pH 1.0. The impedance parameter such as R<sub>ct</sub> and C<sub>dl</sub> values of MWCNT, MWCNT-Co<sub>3</sub>O<sub>4</sub>, MWCNT-NiO, MWCNT-CuO in pH 1.0 media were given in Table 2. The R<sub>ct</sub> values reveal that after modifying with MWCNT/MO composite the resistance was increases because of the passive layer formed by metal oxide. From the Tafel plot (Fig. 9), polarization resistance for the MWCNT and MWCNT/MO coated GCE in pH 1.0 has been estimated by the expression

$$R_p = B/I_{corr}$$

Where  $B = b_a b_c / 2.303(b_a + b_c)$ ,  $b_a$  and  $b_c$  are slopes of the anodic and cathodic plot of the polarization curves.  $I_{corr}$  is the corrosion current. Parameter governing corrosion such as  $R_p$  and  $I_{corr}$  values were calculated and illustrated. From the values it is clear that metal oxide composites are passive to corrosion compared to MWCNT.

**Table 2** R<sub>ct</sub> and C<sub>dl</sub> values of MWCNT and its metal oxide composites

Sample	R <sub>ct</sub> (10 <sup>5</sup> ) (Ωcm <sup>2</sup> )	C <sub>dl</sub> (μFcm <sup>-2</sup> )
MWCNT	0.1954	5.973
MWCNT-Co <sub>3</sub> O <sub>4</sub>	4.165	3.03
MWCNT-NiO	6.309	3.743
MWCNT-CuO	2.462	19.51

**Table 3** Polarization behavior of MWCNT and its metal oxide composites

Sample	I <sub>corr</sub> (10 <sup>-7</sup> )A	R <sub>p</sub> (10 <sup>-8</sup> )
MWCNT	1.912	0.456
MWCNT-Co <sub>3</sub> O <sub>4</sub>	0.4555	0.2032
MWCNT-NiO	1.697	7.81
MWCNT-CuO	1.154	13.06

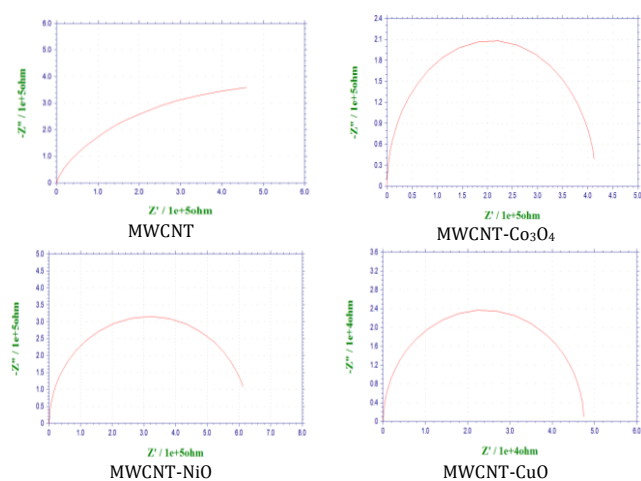


**Fig. 8** Impedance spectrum of MWCNT and MWCNT/MO in pH1.0

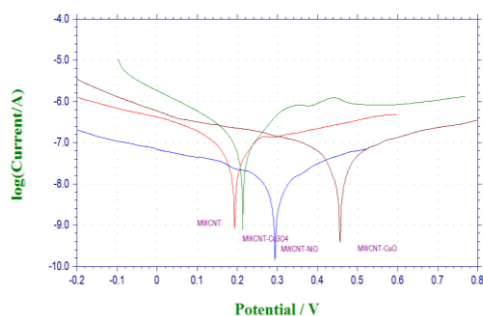


**Fig. 9** Tafel behavior of MWCNT and its metal oxide composites in pH1.0

### 3.6 AFM Spectral Studies

AFM spectra were recorded for the MWCNT-Co<sub>3</sub>O<sub>4</sub>, MWCNT-NiO, MWCNT-CuO thin films on glass substrate. The morphology of the film was studied with AFM under the following conditions: a) scan direction - up, b) Time/Line - 206 ms, c) Tip voltage - 1V, d) Vibration frequency - 169.969 KHz, e) Measurement environment - air and f) Operating mode -

dynamic force. Fig. 10-12 shows the AFM spectral image of MWCNT-Co<sub>3</sub>O<sub>4</sub>, MWCNT-NiO, MWCNT-CuO. The surface shows dis-order manner and presence of metal oxide is confirmed from the spherical particles in the image. The selected particle size of MWCNT-Co<sub>3</sub>O<sub>4</sub>, MWCNT-NiO, MWCNT-CuO were 48 nm, 23 nm and 55 nm respectively.

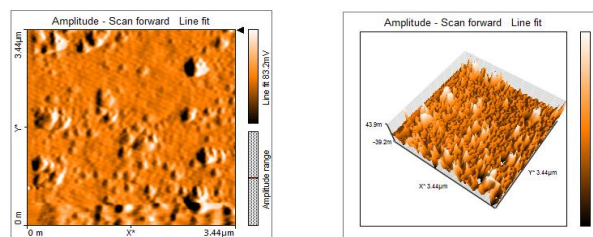


**Fig. 10** AFM image of MWCNT-Co<sub>3</sub>O<sub>4</sub>

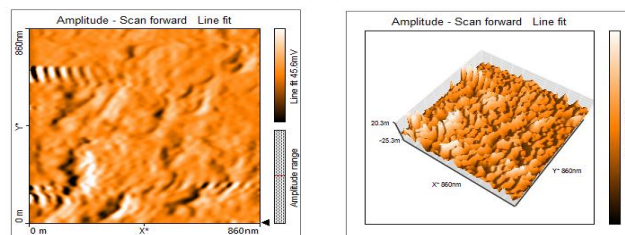


**Fig. 11** AFM image of MWCNT-NiO

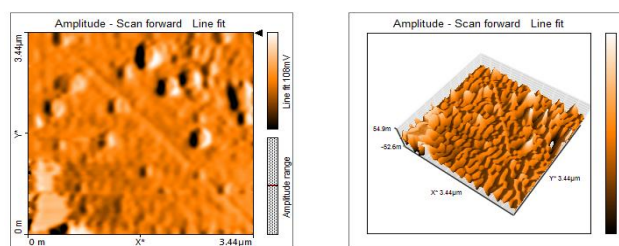


**Fig. 12** AFM image of MWCNT-CuO

## 4. Conclusion

MWCNT have been successfully synthesized by microwave method and MO was incorporated by functionalizing their sidewalls. Then it was characterized by UV-Visible spectroscopy. The band due to  $\pi \rightarrow \pi^*$  was seen at 730 nm. The data obtained from XRD studies coincides well with the JCPDS values of corresponding metal oxides. Cyclic voltammetric studies revealed clearly the redox reaction of MWCNT/MO. From the Tafel plot, polarization resistance of MWCNT/MO in pH 1.0 has been estimated and the values were clear that these composites will be more resistant to corrosion. The AFM photograph shows a spherical growth of metal oxides on the surface of MWCNT.

## Acknowledgement

We gratefully acknowledge Department of Science and Technology (SERC FAST TRACK), and UGC New Delhi, India for providing Electrochemical Work station and FTIR facility.

## References

- [1] S. Iijima, Helical microtubules of graphitic carbon, Nature 354(6348) (1991) 56-58.
- [2] E. Vazquez, V. Georgakilas, M. Prato, Microwave-assisted purification of HIPCO carbon nanotubes, Chem. Comm. 20 (2002) 2308-2309.
- [3] C. Journet, W.K. Maser, P. Bernier, A. Loiseau, M.L. DelaChapelle, S. Lefrant, P. Deniard, R. Lee, J.E. Fischer, Large-scale production of single-walled carbon nanotubes by the electric-arc technique, Nature 388(6644) (1997) 756-758.
- [4] F. Kokai, K. Takahashi, D. Kasuya, T. Ichihashi, M. Yudasaka, S. Iijima, Synthesis of single-wall carbon nanotubes by millisecond-pulsed CO<sub>2</sub> laser vaporization at room temperature, Chem. Phys. Lett. 332(5-6) (2000) 449-454.
- [5] J. Campos-Delgado, I.O. Maciel, D.A. Cullen, D.J. Smith, A. Jorio, M.A. Pimenta, et al., Chemical vapor deposition synthesis of N-, P-, and Si-doped single-walled carbon nanotubes, ACS Nano 4(3) (2010) 1696-1702.

- [6] D. Dallinger, C.O. Kappe, Microwave-assisted synthesis in water as solvent, *Chem. Rev.* 107(6) (2007) 2563-2591.
- [7] F.G. Brunetti, M.A. Herrero, J.D.M. Munoz, S. Giordani, A. Diaz-Ortiz, S. Filippone, et al., Reversible microwave assisted cycloaddition of aziridines to carbon nanotubes, *J. Amer. Chem. Soc.* 129(47) (2007) 14580-14581.
- [8] M. Nuchter, B. Ondruschka, W. Bonrath, A. Gum, Microwave assisted synthesis a critical technology overview, *Green Chem.* 6(2) (2004) 128-141.
- [9] E. Vazquez, M. Prato, Carbon nanotubes and microwaves: interactions, responses, and applications, *ACS Nano* 3(12) (2009) 3819-3824.
- [10] A. Corma, H. García, Supported gold nanoparticles as catalysts for organic reactions, *Chem. Soc. Rev.* 37 (2008) 2096-2126.
- [11] B.Wu, D.Hu, Y. Kuang, B. Liu, X. Zhang, J. Chen, Functionalization of carbon nanotubes by an ionic-liquid polymer dispersion of Pt and Pt-Ru nanoparticles on carbon nanotubes and their electrocatalytic oxidation of methanol, *Angew. Chem. Int. Ed.* 48(26) (2009) 4751-4754.
- [12] Y. Motoyama, M. Takasaki, S.H. Yoon, I. Mochida, H. Nagashima, Rhodium nanoparticles supported on carbon nanofibers as an arene hydrogenation catalyst highly tolerant to a coexisting epoxide group, *Org. Lett.* 11(21) (2009) 5042-5045.
- [13] J. Li, C.Y. Liu, Carbon coated copper nanoparticles synthesis, characterization and optical properties, *New J. Chem.* 33(7) (2009) 1474-1477.
- [14] O. Kharissova, Vertically aligned carbon nanotubes fabricated by microwaves, *Rev. Adv. Mat. Sci.* 7(1) (2004) 50-54.
- [15] V. Veeraputhiran, V. Gomathinayagam, A. Udhaya, K. Francy, B. Kathrunnisa, Microwave Mediated Synthesis and Characterizations of CdO Nanoparticles, *J. Adv. Chem. Sci.* 1(1) (2015) 17-19.
- [16] T. He, R. Chen, X.L. Jiao, Y.L. Wang, Y.Z. Duan, Solubility-Controlled Synthesis of High-Quality Co<sub>3</sub>O<sub>4</sub> Nanocrystals, *Chem. Mater.* 17 (2005) 4023-4030.
- [17] R. Manigandan, K. Giribabu, R. Suresh, L. Vijayalakshmi, A. Stephen, V. Narayanan, Cobalt oxide nanoparticles characterization and its electrocatalytic activity towards nitrobenzene, *Chem. Sci. Trans.* 2(S1) (2013) S47-S50
- [18] K.T. Al-Rasoul, New Method to prepare of NiO nanoparticles by microwaves irradiation, *Asian Trans, Basic. Appl. Sci.* 2(2) (2012) 1-8
- [19] S. Amrut Lanje, J. Satish Sharma, B. Poda Ramachandra, S. Ningthoujam, Synthesis and optical characterization of copper oxide nanoparticles, *Adv. Appl. Sci. Res.* 1(2) (2010) 36-40.